Second ligand-directed self-assembly of lanthanide(III) coordination polymers with 1,4-naphthalenedicarboxylate

Xiang-Jun Zheng,[a] Lin-Pei Jin,*[a] Song Gao[b] and Shao-Zhe Lu[c]

[a] *Department of Chemistry, Beijing Normal University, Beijing, 100875, People's Republic of China. E-mail: lpjin@bnu.edu.cn; Fax: +86-10-58802075; Tel: +86-10-58805522*

[b] *State Key Laboratory of Rare Earth Materials Chemistry and Applications, College of Chemistry and Molecular Engineering, Peking University, Beijing, 100871, People's Republic of China*

[c] *Laboratory of Excited State Processes, Chinese Academy of Sciences, Changchun Institute of Optics, Fine Mechanics and Physics, Chinese Academy of Sciences, Changchun, 130021, People's Republic of China*

Under hydrothermal conditions, 1,4-naphthalenedicarboxylic acid (H_2NDC) reacts with lanthanide(III) chloride to form the coordination polymers $[Ln_2(NDC)_3(H_2O)_2] \cdot nH_2O$ [$n = 2$, Ln = Eu (**1**); $n = 1.5$, Ln = Gd (**2**)]. If a second ligand, 4,4′-bipyridine (4,4′-bpy), is added to the reaction mixture, the coordination polymers $[Ln_2(NDC)_3(4,4′-bpy)_{0.5}(H_2O)_3] \cdot (4,4′-bpy)$ [Ln = Eu (**3**); Ln = Yb (**4**)] are obtained. **1** and **2** are isostructural and they possess a porous 3D network with the lanthanide(III) ions bridged only by NDC anions. **3** and **4** are unprecedented lanthanide coordination polymers of polycarboxylate with 4,4′-bpy. They possess a 3D porous structure assembled by lanthanide ions with the linkers NDC and 4,4′-bpy, while lattice molecules of 4,4′-bpy are enclathrated in the cavities. The photophysical properties of **3** and the magnetic properties of **2** were investigated, and the thermogravimetric analyses of **1** and **3** were also carried out.

Introduction

The assembly of porous networks has been an intriguing field as these systems have potential applications in catalysis,[1,2] adsorption and separation processes,[3–9] ion exchange,[10,11] and sensor technology.[12,13] Many molecular-based porous materials constructed by coordination polymers have been reported.[6–9,14–19] These coordination polymers with open frameworks possess unprecedented pore sizes, shapes and functions. In constructing the open frameworks, organic linkers such as polycarboxylic acids, especially linear dicarboxylic acids, are frequently utilized because they may act as both counteranions and bridging ligands to extend the architecture to different dimensions.

1,4-Naphthalenedicarboxylic acid (NDC) is a rigid linear bifunctional ligand. Its coordination polymers with transition metal ions have been reported.[20,21] We have obtained two heptanuclear lanthanide hydroxo clusters of the dicubane-like type, which were used as a secondary building unit to form a 3D framework through linkage of NDC.[22] Apart from these, no other lanthanide coordination polymers of NDC have been reported. 4,4′-Bipyridine (4,4′-bpy) is a neutral linear bifunctional ligand, widely used as an excellent spacer in the construction of transition metal coordination polymers of carboxylates.[23–30] However, for its lanthanide analogs, there are only two reports on the lanthanide complexes of monocarboxylates with 4,4′-bpy,[31,32] and to the best of our knowledge, no lanthanide complex of a polycarboxylate with 4,4′-bpy is documented because it is difficult for 4,4′-bpy to coordinate with Ln(III) ions directly.

On one hand, compared with transition metals, lanthanides have relatively high coordination numbers. To complete the coordination sphere, small solvent molecules such as H_2O find it much easier to occupy the coordination sites than 4,4′-bpy, due to the steric effect. On the other hand, according to the hard-soft acid-base theory, 4,4′-bpy is a soft base, while lanthanide is a hard acid having a relatively high affinity for hard bases such as oxygen-containing carboxylate and 4,4′-bipyridine-*N*, *N*′-dioxide ligands.[33,34] But once 4,4′-bpy is introduced, NDC and 4,4′-bpy can both act as long bridging ligands and both are of similar length (*ca.* 7.0 Å), which facilitates the construction of a square structure with a large pore size. The typical bis(monodentate) coordination mode of 4,4′-bpy will affect the coordination mode of NDC and consequently change the framework of the resulting coordination polymers. In addition, NDC and 4,4′-bpy are a combination of neutral and anionic linkers, obviating the need for counterions in the cavities when constructing porous coordination polymers. In the present work, the second-ligand-directed self-assembly of lanthanide(III) coordination polymers with dicarboxylate NDC is reported, especially the synthesis and structures of the first examples of porous lanthanide coordination polymers formed by NDC and 4,4′-bpy through hydrothermal synthesis.

Experimental

General remarks

$LnCl_3 \cdot 6H_2O$ (Ln = Eu, Gd, Yb) were prepared by dissolving their oxides in concentrated hydrochloric acid and then evaporating the solvents to dryness. All of the other reagents were commercially available and used without further purification. Elemental analyses were obtained on an Elementar Vario EL analyzer. The IR spectra were recorded with a Nicolet Avatar 360 FT-IR spectrometer using the KBr pellet technique. Thermogravimetric analyses were performed with a ZRY-2P Thermal Analyzer. The magnetic susceptibilities were obtained on a

Table 1 Crystallographic data for compounds **1–4**

	1	**2**	**3**	**4**
Empirical formula	$C_{36}H_{26}Eu_2O_{16}$	$C_{36}H_{25}Gd_2O_{15.50}$	$C_{51}H_{36}Eu_2N_3O_{15}$	$C_{51}H_{36}N_3O_{15}Yb_2$
Formula weight	1018.49	1020.06	1234.75	1276.91
Temperature/K	293(2)	293(2)	293(2)	293(2)
Wavelength/Å	0.71073	0.71073	0.71073	0.71073
Crystal system	Tetragonal	Tetragonal	Monoclinic	Monoclinic
Space group	$I4_1cd$	$I4_1cd$	$P2_1/n$	$P2_1/n$
$a/Å$	30.392(4)	30.408(5)	14.240(5)	14.099(5)
$b/Å$	30.392(4)	30.408(5)	22.191(7)	21.938(8)
$c/Å$	15.737(4)	15.747(5)	15.185(5)	15.066(6)
$α/°$	90	90	90	90
$β/°$	90	90	102.980(5)	103.259(8)
$γ/°$	90	90	90	90
$U/Å^3$	14 535(5)	14 560(6)	4676(2)	4536(3)
Z	16	16	4	4
D_c/g cm^{-3}	1.862	1.861	1.754	1.870
$μ$/mm^{-1}	3.495	3.685	2.734	4.176
Reflections collected	36 344	40 403	19 567	23 444
Unique reflections	6336	7351	8160	7978
R_{int}	0.0915	0.0723	0.0689	0.2936
$R_1 [I > 2σ(I)]$	0.0387	0.0362	0.0423	0.0959
$wR_2 [I > 2σ(I)]$	0.0586	0.0548	0.0557	0.1728
R_1 (all data)	0.0679	0.0650	0.0845	0.2442
wR_2 (all data)	0.0657	0.0623	0.0645	0.2582

crystal sample using an Oxford MagLab System 2000 magnetometer. The experimental susceptibilities were corrected for the sample holder and the diamagnetism contributions estimated from Pascal's constants.

Syntheses

$[Eu_2(NDC)_3(H_2O)_2] \cdot 2H_2O$ (1). A mixture of H_2O (5 ml), aqueous NaOH (0.44 ml, 0.29 mmol), $EuCl_3 \cdot 6H_2O$ (0.037 g, 0.1 mmol) and 1,4-naphthalenedicarboxylic acid (0.033 g, 0.15 mmol) was sealed in a 25 ml stainless reactor with a Teflon liner and heated at 120 °C for 72 h. Yellow crystals of **1** were obtained in a yield of 0.025 g (49%). Anal calcd for $C_{36}H_{26}Eu_2O_{16}$ (1018.49): C, 42.45; H, 2.57. Found: C, 42.15; H, 2.37%. IR data: $ν$/cm^{-1} 3443 s, 1616 m, 1560 m, 1527 m, 1462 m, 1417 s, 1363 s, 1346 m, 1257 m, 842 m, 784 m.

$[Gd_2(NDC)_3(H_2O)_2] \cdot 1.5H_2O$ (2). For this compound the same procedure as that for **1** was followed, using $GdCl_3 \cdot 6H_2O$ (0.037 g, 0.1 mmol). Yellow crystals of **2** were obtained in a yield of 0.024 g (47%). Anal calcd for $C_{36}H_{25}Gd_2O_{15.5}$ (1020.06): C, 42.39; H, 2.47. Found: C, 42.15; H, 2.19%. IR data: $ν$/cm^{-1} 3442 s, 1701 m, 1560 m, 1516 m, 1466 m, 1419 m, 1370 s, 1267 m, 848 w, 783 w.

$[Eu_2(NDC)_3(4,4'-bpy)_{0.5}(H_2O)_3] \cdot (4,4'-bpy)$ (3). A mixture of H_2O (2 ml), aqueous NaOH (0.44 ml, 0.29 mmol), $EuCl_3 \cdot 6H_2O$ (0.037 g, 0.1 mmol), 1,4-naphthalenedicarboxylic acid (0.033 g, 0.15 mmol), $NaAc \cdot 3H_2O$ (0.01 g, 0.07 mmol), and $4,4'-bpy \cdot 2H_2O$ (0.02 g, 0.1 mmol) was sealed in a 25 ml stainless reactor with a Teflon liner and heated at 120 °C for 48 h. Yellow crystals of **3** were obtained in a yield of 0.029 g (47%). Anal calcd for $C_{51}H_{36}Eu_2N_3O_{15}$ (1234.75): C, 49.61; H, 2.94; N, 3.40. Found: C, 50.13; H, 3.26; N, 3.10%. IR data: $ν$/cm^{-1} 3418 s, 1601 s, 1573 s, 1532 s, 1463 s, 1422 s, 1366 s, 1264 m, 842 s, 799 m, 785 m, 576 m.

$[Yb_2(NDC)_3(4,4'-bpy)_{0.5}(H_2O)_3] \cdot (4,4'-bpy)$ (4). For this compound the same procedure as that for **3** was followed, using $YbCl_3 \cdot 6H_2O$ (0.037 g, 0.1 mmol). Yellow crystals of **4** were obtained in a yield of 0.02 g (31%). Anal calcd for $C_{51}H_{36}N_3O_{15}Yb_2$ (1276.91): C, 47.97; H, 2.84; N, 3.29. Found:

C, 47.88; H, 2.65; N, 3.26%. IR data: $ν$/cm^{-1} 3427 s, 1595 s, 1534 s, 1465 s, 1427 s, 1369 s, 1266 m, 845 s, 796 m, 781 m, 566 m.

High-resolution luminescence spectra

The excitation light source was a Nd:YAG laser, which emits at 1.064 μm; the excitation wavelength was 355 nm. The sample was placed in a Dewar bottle and cooled with liquid nitrogen. The fluorescence was collected at right angles through a Spex 1403 monochromator and a photomultiplier tube (Japan, R955), then averaged with a boxcar integrator (America, EG 162) and finally data were transferred to a computer.

X-Ray crystallography†

The X-ray single-crystal data collections for complexes **1–4** were performed on a Bruker Smart 1000 CCD diffractometer, using graphite-monochromated Mo-Kα radiation ($λ$ = 0.710 73 Å). Semiempirical absorption corrections were applied using the SADABS program. The structures were solved by direct methods and refined by full-matrix least-squares methods on F^2 using the SHELXTL-97 program. All non-hydrogen atoms were refined with anisotropic displacement parameters. The hydrogen atoms were generated geometrically and treated by a mixture of independent and constrained refinements. Experimental details for the X-ray data collection of **1–4** are presented in Table 1, while selected bond distances for **1–4** are listed in Table 2.

Results and discussion

Crystal structures

All of the compounds are stable in air and insoluble in water and in common organic solvents. High yields of the target compounds indicate that these compounds are thermodynamically stable under the prevailing reaction conditions. Given that **1** and **2** are isostructural, only the structure of complexes **1**, **3** and **4** will be discussed here.

---

† CCDC reference numbers 245416–245419. See http://www.rsc.org/suppdata/nj/b4/b415337e/ for crystallographic data in .cif or other electronic format.

Table 2   Selected bond distances (Å) in compounds **1–4**[a]

1

Eu(1)–O(9)	2.331(6)	Eu(1)–O(14)	2.508(6)	Eu(2)–O(3)#3	2.450(6)
Eu(1)–O(4)#1	2.400(5)	Eu(1)–O(1)	2.585(6)	Eu(2)–O(8)#1	2.466(5)
Eu(1)–O(2)	2.403(5)	Eu(1)–O(3)#1	2.586(5)	Eu(2)–O(11)#4	2.483(5)
Eu(1)–O(13)	2.409(5)	Eu(2)–O(10)	2.349(6)	Eu(2)–O(5)	2.497(5)
Eu(1)–O(12)#2	2.438(6)	Eu(2)–O(6)	2.404(6)	Eu(2)–O(12)#4	2.577(5)
Eu(1)–O(7)#1	2.458(6)	Eu(2)–O(1)	2.422(6)	Eu(2)–O(7)#1	2.687(6)

2

Gd(1)–O(9)	2.304(6)	Gd(1)–O(14)	2.499(6)	Gd(2)–O(3)#3	2.428(6)
Gd(1)–O(2)	2.382(4)	Gd(1)–O(3)#1	2.601(5)	Gd(2)–O(8)#1	2.456(4)
Gd(1)–O(13)	2.392(5)	Gd(1)–O(1)	2.607(5)	Gd(2)–O(11)#4	2.472(5)
Gd(1)–O(4)#1	2.408(5)	Gd(2)–O(10)	2.325(6)	Gd(2)–O(5)	2.479(5)
Gd(1)–O(12)#2	2.418(5)	Gd(2)–O(1)	2.394(5)	Gd(2)–O(12)#4	2.558(5)
Gd(1)–O(7)#1	2.424(6)	Gd(2)–O(6)	2.399(5)	Gd(2)–O(7)#1	2.709(6)

3

Eu(1)–O(1)	2.312(4)	Eu(1)–O(6)	2.505(4)	Eu(2)–O(12)#6	2.417(4)
Eu(1)–O(9)	2.408(4)	Eu(1)–N(3)	2.632(5)	Eu(2)–O(5)	2.419(4)
Eu(1)–O(13)	2.409(4)	Eu(1)–O(5)	2.744(4)	Eu(2)–O(4)#7	2.424(4)
Eu(1)–O(14)	2.436(4)	Eu(2)–O(2)	2.339(4)	Eu(2)–O(10)	2.446(4)
Eu(1)–O(8)#5	2.443(4)	Eu(2)–O(15)	2.381(4)	Eu(2)–O(3)#7	2.567(4)
Eu(1)–O(7)#5	2.484(4)	Eu(2)–O(11)#6	2.402(4)	Eu(2)–O(9)	2.825(4)

4

Yb(1)–O(8)	2.213(19)	Yb(1)–O(2)	2.48(2)	Yb(2)–O(10)#8	2.330(18)
Yb(1)–O(11)	2.298(18)	Yb(1)–N(1)	2.554(19)	Yb(2)–O(9)#8	2.333(18)
Yb(1)–O(14)	2.332(16)	Yb(2)–O(7)	2.232(17)	Yb(2)–O(5)#9	2.343(15)
Yb(1)–O(13)	2.337(19)	Yb(2)–O(4)#8	2.288(18)	Yb(2)–O(12)	2.346(18)
Yb(1)–O(1)	2.369(17)	Yb(2)–O(15)	2.306(17)	Yb(2)–O(6)#9	2.519(16)
Yb(1)–O(3)#8	2.386(17)				

[a] Symmetry codes are given by: #1 $-y + 1$, $-x + 1/2$, $z - 1/4$; #2 $-y + 1/2$, $x + 0$, $z - 1/4$; #3 $y + 0$, $-x + 1/2$, $z + 1/4$; #4 $y + 1/2$, x, $z + 1/4$; #5 $x - 1/2$, $-y + 3/2$, $z + 1/2$; #6 $x + 1/2$, $-y + 3/2$, $z - 1/2$; #7 $-x + 3/2$, $y + 1/2$, $-z + 3/2$; #8 $x + 1/2$, $-y + 1/2$, $z - 1/2$; #9 $-x + 3/2$, $y - 1/2$, $-z + 1/2$.

The asymmetric unit of **1** consists of a binuclear unit, $[Eu_2(NDC)_3(H_2O)_2] \cdot 2H_2O$. There are two crystallographic different Eu(III) ions although they are both nine-coordinate with oxygen atoms (Fig. 1). Eu1 is bonded to seven oxygen atoms (O1, O2, O3A, O4A, O7A, O9, O12A) from five NDC anions and two oxygen atoms (O13, O14) from two water molecules, while Eu2 is bound only to carboxylate oxygen atoms (O1, O3B, O5, O6, O7A, O8A, O10, O11B, O12B) from six NDC anions, resulting in different coordination environment from that of Eu1. The NDC anions in **1** adopt three coordination modes, labelled **a**, **b**, **c** in Scheme 1. In **1**, the bridging ligand NDC orients in two directions, [110] and [1 1̄0], linking the Eu(III) ions in these two directions, to form a square grid in the (001) plane with a dimension of 10.7×10.7 Å^2
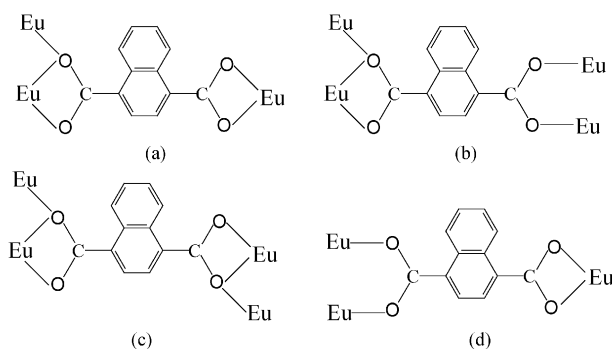
Scheme 1   Coordination modes of NDC ligand in the complexes **1** and **3**.

(Fig. 2). Every grid contains eight Eu(III) ions and every vertex comprises two crystallographically different Eu(III) ions with an Eu···Eu distance of 3.99 Å. In the c axis direction, the Eu(III) ions are bridged by one carboxylate group of every NDC anion (Fig. 3). Adjacent grids are linked through the chelating-bridging tridentate carboxylate group of the NDC anions that adopt coordination modes **b** and **c**. The Eu···Eu distance between adjacent grids is 4.19 Å. In this fashion, compound **1** forms a 3D open framework with 1D square channels. However, the channels are partially occupied by the bulky naphthalene rings of the NDC ligands. The lattice water molecules are hydrogen-bonded to the coordinating water molecules through O–H···O hydrogen bonds and are enclathrated in the cavities between naphthalene rings (Fig. 4). The lattice waters in the neighboring cavities are not coplanar, but are located near the two groups on opposite sides of the square channel. These lattice water molecules contribute to the stabilization of the crystal structure.

The asymmetric unit of **3** consists of a binuclear unit, $[Eu_2(NDC)_3(4,4'\text{-bpy})_{0.5}(H_2O)_3] \cdot (4,4'\text{-bpy})$. The two Eu(III) ions are both nine-coordinate but they are in obviously different coordination environments (Fig. 5). Eu1 is surrounded by four NDC anions, two water molecules and one 4,4'-bpy molecule, while Eu2 is surrounded by five NDC anions and one water molecule. In the crystal of **3**, NDC and 4,4'-bpy both act as linkers to arrange the Eu(III) ions. 4,4'-bpy adopts a bis(monodentate) mode, while NDC adopts two types of coordination modes, **a** and **d** in Scheme 1. The naphthalene rings of the NDC ligands adopting the **d** coordination mode and displaying the same orientation, are partly overlapped
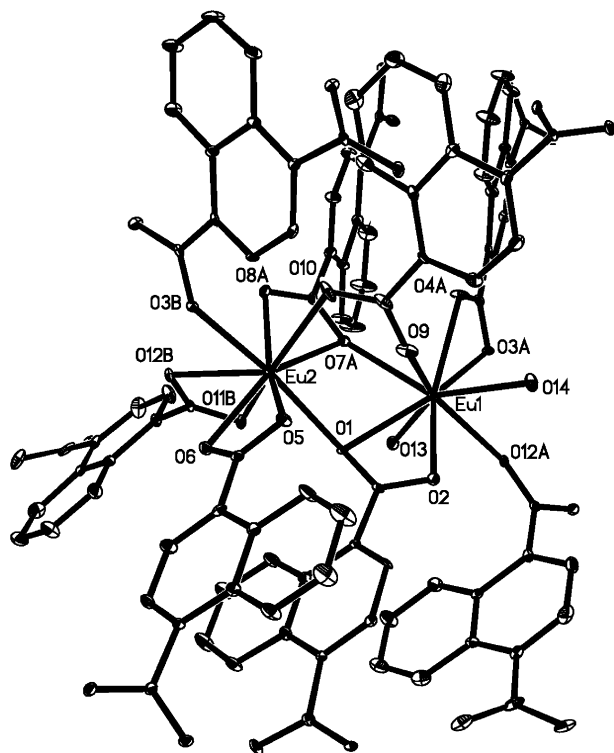
Fig. 1 Coordination environment of Eu^{3+} ions in **1**. The related coordination atoms are labelled. Lattice molecule and all hydrogen atoms are omitted for clarity. Thermal ellipsoids are shown at 10% probability.

with a dihedral angle of 3.6° and an interplanar distance of about 3.4 Å, indicating a π–π stacking interaction between them. The two pyridine rings of the coordinating 4,4′-bpy are coplanar, while those of the lattice one are not coplanar (dihedral angle of 38.4°). The framework structure of **3** is built-up from the binuclear $Eu_2(NDC)_3(4,4'\text{-bpy})_{0.5}(H_2O)_3$ unit. First, in the (1 0 1̄) plane, two NDC anions, which adopt coordination mode **d**, together with one 4,4′-bpy molecule, orient in the three directions, respectively (Fig. 6). Every binuclear unit is connected by these three ligands with three adjacent binuclear units in the (1 0 1̄) plane. These connections result in a 62-membered ring comprising 8 Eu, 38 C, 4 N and 12 O atoms. Regarding every binuclear unit as a node, the
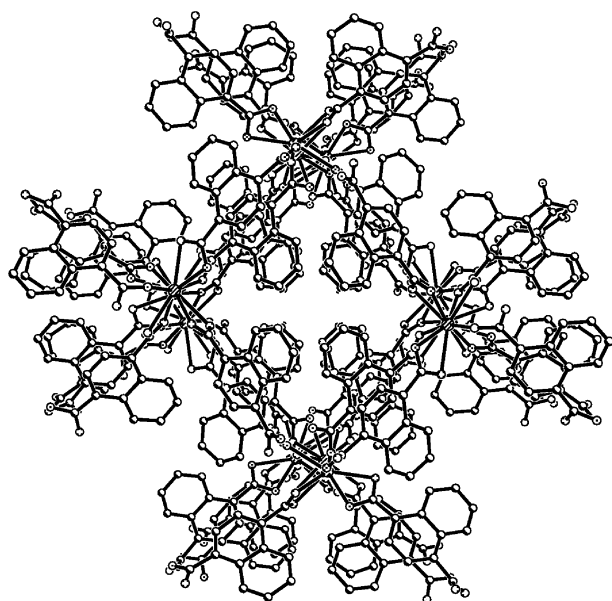
Fig. 2 Cross-section of the 1D channel in the structure of **1**.
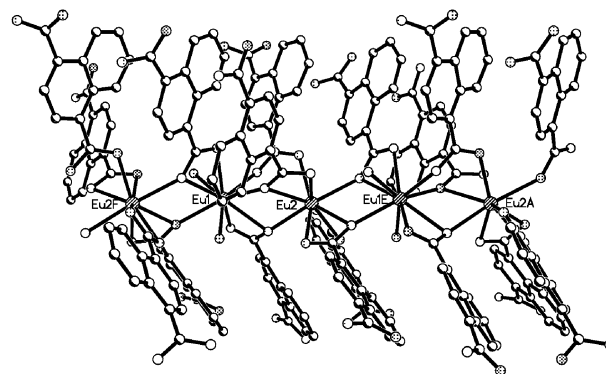
Fig. 3 The linking of Eu(III) ions in **1** along the *c* axis.

62-membered ring can be seen as a parallelogram; the midpoint of the long side consists of a binuclear unit. The extended structure in the (1 0 1̄) plane is a herringbone architecture (Fig. 6). Four NDC anions adopting coordination mode **a** connect the binuclear unit with two adjacent ones in the [1 0 1̄] direction, resulting in a 3D metal-organic framework with a grid architecture. The 3D framework contains many cavities in which guest molecules of 4,4′-bpy are accommodated (Fig. 7) through O–H···N hydrogen bonding to the coordinating water molecules. The two nitrogen atoms of the guest 4,4′-bpy are arrayed in the diagonal direction of the parallelogram channel. The appropriate length of two types of linkers, the rigidity of the naphthalene ring, and the π–π stacking and hydrogen-bonding interactions probably contribute to the resulting framework and accordingly the formation of compound **3**.

Compound **4** contains two crystallographically independent Yb(III) ions, both of which are eight-coordinate, in contrast to the Eu(III) ions in **3**, which are nine-coordinate. This can be ascribed to the effect of lanthanide contraction. In **4** the ligand NDC adopts only the bridging bidentate and chelating bidentate coordination modes. It is noteworthy that although **3** and **4** have different coordination numbers and coordination modes, they finally construct similar 3D architectures, as shown in Fig. 7.

Compounds **1** and **3** both contain the NDC anion, which acts as a linker to connect different Eu^{3+} ions. The induction of a second ligand, 4,4′-bpy, changes the self-assembly of Eu^{3+} and NDC. In compound **1**, the NDC anion has three complicated coordination modes; it orients vertically in two directions, linking the Eu^{3+} ions in these directions to form a square grid with dimensions of 10.7 × 10.7 Å². In the other direction, the Eu^{3+} ions are linked *via* the bridging carboxylate, not the
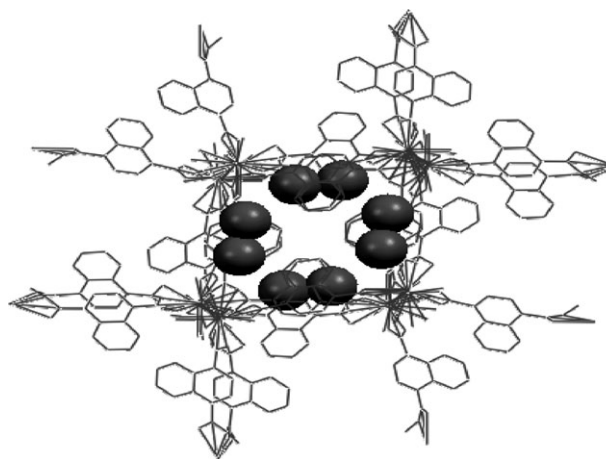

Fig. 4 3D metal-organic framework of **1**, showing the cavities occupied by lattice water molecules, which are displayed with a space-filling model. All hydrogen atoms are omitted for clarity.
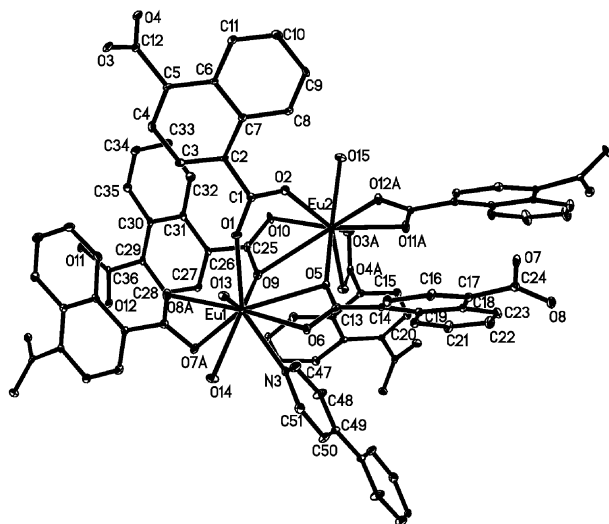
Fig. 5 Coordination environment of Eu^{3+} ions in **3**. The asymmetric unit and the related coordination atoms are labelled. Lattice molecule and all hydrogen atoms are omitted for clarity. Thermal ellipsoids are shown at 10% probability.

Fig. 7 3D grid architecture of **3** viewed along the [1 0 1] direction. The 4,4′-bpy lattice molecules are displayed with a space-filling model.

entire NDC anion, giving rise to a small $Eu^{3+} \cdots Eu^{3+}$ separation (average 4.1 Å) in this direction. Thus, a 3D structure with a 1D channel is obtained. However, most of the channel is occupied by the bulky naphthalene rings of the coordinating NDC anions. Only small lattice water molecules can be accommodated between the naphthalene rings in the 1D channel, resulting in a host-guest compound.

In compound **3**, although the NDC anion adopts simple coordination modes and the number of coordination modes decreases, the coordination number of Eu^{3+} remains unchanged because of the addition of 4,4′-bpy. In **3** the NDC anion orients in three directions, with 4,4′-bpy alternating with the NDC anion in one direction. The Eu^{3+} ions in the three directions are linked *via* bridging of the entire NDC anion or 4,4′-bpy, giving rise to a large $Eu^{3+} \cdots Eu^{3+}$ separation in the framework. The cross-section of the 1D channel (Fig. 7) has dimensions of 11.5×11.1 Å^2, and the $Eu^{3+} \cdots Eu^{3+}$ separation perpendicular to this plane is 9.2 Å. As in compound **1** the

bulky naphthalene rings of coordinating NDC anions are located in the 1D channel. But, owing to the long distance between Eu^{3+} ions, the large lattice molecule 4,4′-bpy can be accommodated in the cavities between the naphthalene rings. Therefore, 4,4′-bpy plays an important role in constructing a lanthanide-organic framework having a large pore size.

Photophysical properties

Eu(III) ion is frequently used as a structural probe to investigate local symmetry.[35] The lowest emission level $^5D_0$ and the ground state $^7F_0$ are both nondegenerate. Therefore, the number of excitation peaks corresponding to the $^7F_0 \rightarrow {}^5D_0$ transition will reveal the number of Eu(III) ions with different coordination environments in the compound. Compound **3** displays intense luminescence upon excitation. Fig. 8(a) and 8(b) illustrate the emission spectra of **3** excited with 355 nm at
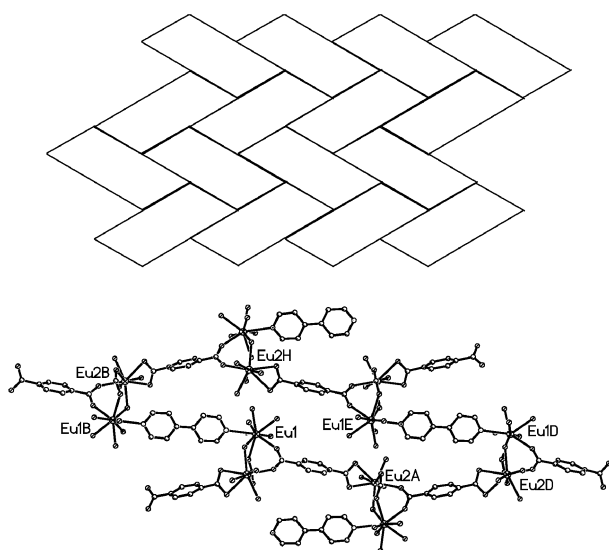

Fig. 6 (top) 2D herringbone architecture in the (1 0 $\bar{1}$) plane constructed by Eu(III) ions, 4,4′-bpy and NDC anions adopting coordination mode **d** in Scheme 1. (bottom) The subunit of a 62-membered parallelogram with 8 Eu, 38 C, 4 N and 12 O atoms in **3**. The chemical structure of 1,4-naphthalenedicarboxylate is abbreviated to *p*-phthalate and all hydrogen atoms are omitted for clarity.
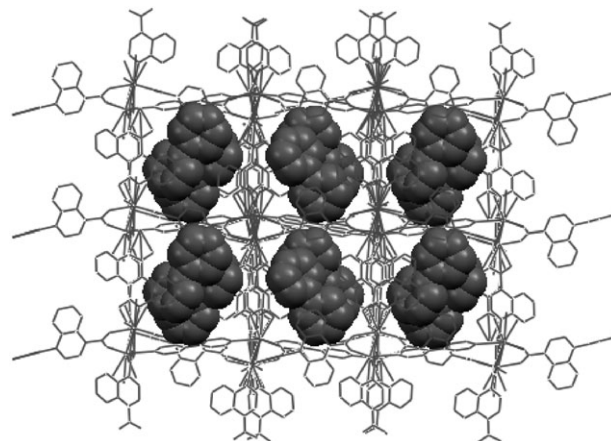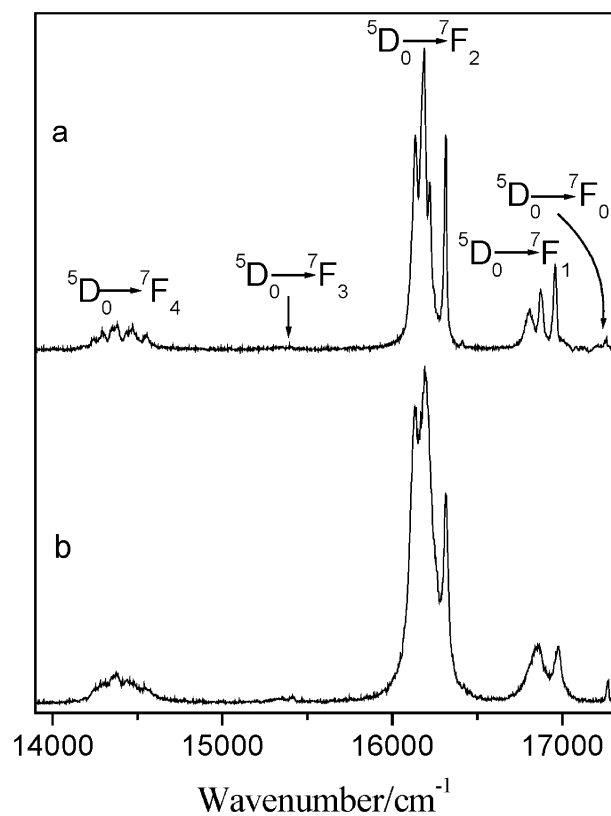

Fig. 8 Emission spectra of **3** corresponding to the $^5D_0 \rightarrow {}^7F_J$ (J = 0–4) transitions at (a) 77 and (b) 293 K; λ_{exc} = 355 nm.
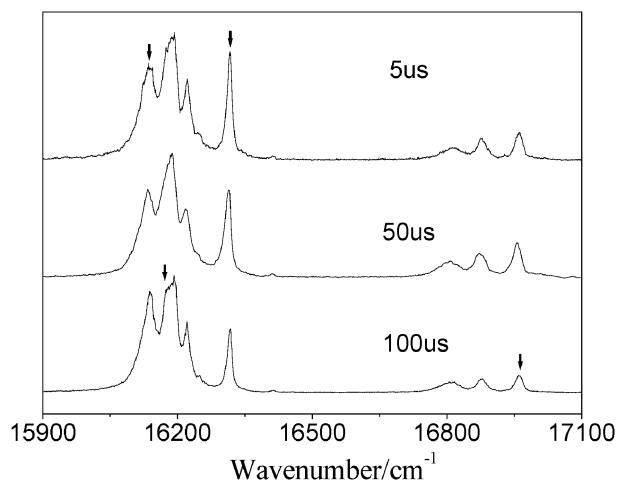
Fig. 9 Time-resolved spectra of **3** at 77 K in the range of 17 100–15 900 cm^{-1}; delay times: 5, 50 and 100 µs; λ_{exc} = 355 nm.

77 and 293 K, respectively, corresponding to $^5D_0 \to {}^7F_J$ (J = 0–4) transitions. The intensity ratios $^5D_0 \to {}^7F_2/{}^5D_0 \to {}^7F_1$ = 4.1 (a) and 5.8 (b) show that Eu(III) ions are not at inversion centers. The emission peaks in Fig. 8(a) show line-narrowing at 77 K and thus become more developed. No obvious and direct information about the Eu^{3+} ion sites can be obtained from Fig. 8, but from the time-resolved spectra (Fig. 9) corresponding to the $^5D_0 \to {}^7F_J$ (J = 1, 2) transitions, it can be seen that the shape or the relative intensity (as denoted by ↓) of the peaks apparently change with the applied time delay. It can be concluded that there is more than one Eu(III) ion site in **3**. Selective excitation techniques were applied to further probe the number of Eu(III) ion sites in compound **3**. The excitation spectra (Fig. 10) of **3** were recorded at 77 and 293 K, setting
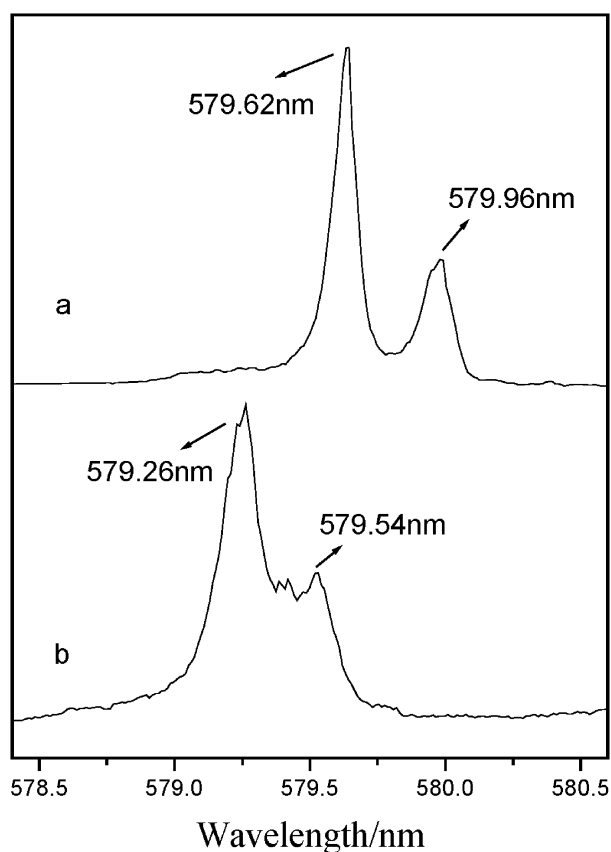

Fig. 10 Excitation spectra of **3** at (a) 77 and (b) 293 K; analysis wavenumber is (a) 16 185 or (b) 16 155 cm^{-1}.
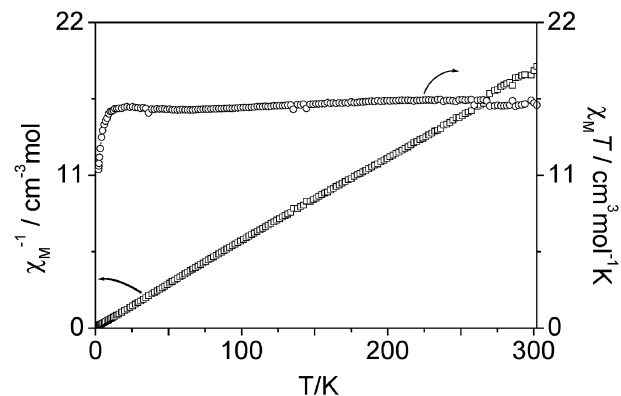

Fig. 11 Plot of the temperature dependence of $\chi_M T$ (O) and χ_M^{-1} (□) for **2** (per [Gd]$_2$ unit).

16 185 and 16 155 cm^{-1}, respectively, as the analysis wavenumber. The excitation bands in Fig. 10(b) are blue-shifted compared with those in Fig. 10(a), which may be due to the phonon effect of lattice thermal vibrations on the energy levels. The spectrum at 77 K is more resolved, with narrower lines, than that at 293 K. Fig. 10(a) is composed of two components with peak positions at 579.62 and 579.96 nm. This means that there exists two Eu(III) ion sites in **3**, which is in good agreement with the result of the single-crystal X-ray diffraction analysis. However, broad emission spectra similar to Fig. 8(a) were obtained when exciting at 579.62 and 579.96 nm at 77 K. This may be due to energy transfer between Eu(III) ion sites, which is a common phenomenon in europium coordination polymers.

Magnetic properties of 2

For **2**, the observed $\chi_M T$ value per [Gd]$_2$ unit is 16.04 cm^3 K mol^{-1} at room temperature (Fig. 11), close to the expected value of 15.76 cm^3 K mol^{-1} for two magnetically isolated S = 7/2 local spins with g = 2.0 Gd(III) ion.[36] The $\chi_M T$ value remains almost constant to *ca.* 11 K (15.60 cm^3 K mol^{-1}), then drops sharply below 11 K to 11.41 cm^3 K mol^{-1} at 2 K. The plot of χ_M^{-1} *vs.* T in the temperature range of 40–300 K obeys the Curie–Weiss law [χ = $C/(T - \theta)$] with C = 16.43 cm^3 K mol^{-1} and θ = −2.66 K. The decrease of $\chi_M T$ or the small negative θ is primarily attributed to the possible very weak antiferromagnetic coupling between the Gd^{3+} ions in **2**. The shortest distance between two Gd^{3+} ions appears to be large (4.03 Å), which precludes effective coupling between Gd^{3+} ions. It turns out that the dipolar couplings are, indeed, small since the θ value is quite small.

Thermal stability analysis

Considering that compounds **1** and **2** are isostructural and that compounds **3** and **4** have similar 3D structure, compounds **1** and **3** were taken as examples to investigate the thermal stability by thermogravimetric analysis. For compound **1**, the first weight loss of 6.4% from 83 to 232 °C corresponds to the loss of two lattice water molecules and two coordinating water molecules (calcd: 7.1%), leaving a framework of [Eu$_2$(NDC)$_3$]. [Eu$_2$(NDC)$_3$] remained stable up to 370 °C at which point it began to decompose. Compound **3** underwent a first weight loss of 11.5% from 145 to 274 °C, corresponding to the loss of one lattice 4,4′-bpy molecule (calcd: 12.6%), leaving a framework of [Eu$_2$(NDC)$_3$(4,4′-bpy)$_{0.5}$(H$_2$O)$_3$]. This framework began to decompose at 355 °C and ends at 641 °C with in 29.2% of the residue Eu$_2$O$_3$ obtained (calcd: 28.5%).

Acknowledgements

References

1   J. S. Seo, D.-M. Whang, H.-Y. Lee, S. I. Jun, J.-H. Oh, Y.-J. Jeon and K.-M. Kim, *Nature (London)*, 2000, **404**, 982–986.
2   T. Sawaki and Y. Aoyama, *J. Am. Chem. Soc.*, 1999, **121**, 4793–4798.
3   H. Li, M. Eddaoudi, M. O'Keeffe and O. M. Yaghi, *Nature (London)*, 1999, **402**, 276–279.
4   S.-I. Noro, S. Kitagawa, M. Kondo and K. Seki, *Angew. Chem., Int. Ed.*, 2000, **39**, 2082–2084.
5   H. J. Choi, T. S. Lee and M. P. Suh, *Angew. Chem., Int. Ed.*, 1999, **38**, 1405–1408.
6   M. P. Suh, J. W. Ko and H. J. Choi, *J. Am. Chem. Soc.*, 2002, **124**, 10976–10977.
7   A. Dimos, D. Tsaousis, A. Michaelides, S. Skoulika, S. Golhen, L. Ouahab, C. Didierjean and A. Aubry, *Chem. Mater.*, 2002, **14**, 2616–2622.
8   E. J. Cussen, J. B. Claridge, M. J. Rosseinsky and C. J. Kepert, *J. Am. Chem. Soc.*, 2002, **124**, 9574–9581.
9   M. Eddaoudi, J. Kim, N. Rosi, D. Vodak, J. Wachter, M. O'Keeffe and O. M. Yaghi, *Science*, 2002, **295**, 469–472.
10 K. S. Min and M. P. Suh, *J. Am. Chem. Soc.*, 2000, **122**, 6834–6840.
11 O. M. Yaghi and H. Li, *J. Am. Chem. Soc.*, 1996, **118**, 295–296.
12 M. Albrecht, M. Lutz, A. L. Spek and G. van Koten, *Nature (London)*, 2000, **406**, 970–974.
13 J. A. Real, E. Andrés, M. C. Muñoz, M. Julve, T. Granier, A. Bousseksou and F. Varret, *Science*, 1995, **268**, 265–267.
14 J. W. Ko, K. S. Min and M. P. Suh, *Inorg. Chem.*, 2002, **41**, 2151–2157.
15 L. Pan, K. M. Adams, H. E. Hernandez, X. T. Wang, C. Zheng, Y. Hattori and K. Kaneko, *J. Am. Chem. Soc.*, 2003, **125**, 3062–3067.
16 Y.-H. Liu, Y.-L. Lu, H.-C. Wu, J.-C. Wang and K.-L. Lu, *Inorg. Chem.*, 2002, **41**, 2592–2597.
17 P. Ayyappan, O. R. Evans and W. B. Lin, *Inorg. Chem.*, 2001, **40**, 4627–4632.
18 S. Kitagawa, R. Kitaura and S.-i. Noro, *Angew. Chem., Int. Ed.*, 2004, **43**, 2334–2375.
19 X. J. Zheng, Z. M. Wang, S. Gao, F. H. Liao, C. H. Yan and L. P. Jin, *Eur. J. Inorg. Chem.*, 2004, 2968–2973.
20 D. T. Vodak, M. E. Braun, J. Kim, M. Eddaoudi and O. M. Yaghi, *Chem. Commun.*, 2001, 2534–2535.
21 J. Y. Lu and V. Schauss, *CrystEngComm*, 2002, **4**, 623–625.
22 X. J. Zheng, L. P. Jin and S. Gao, *Inorg. Chem.*, 2004, **43**, 1600–1602.
23 Y. Rodriguez-Martin, C. Ruiz-Perez, J. Sanchiz, F. Lloret and M. Julve, *Inorg. Chim. Acta*, 2001, **318**, 159–165.
24 J. Tao, Y. Zhang, M. L. Tong, X. M. Chen, T. Yuen, C. L. Lin, X. Y. Huang and J. Li, *Chem. Commun.*, 2002, 1342–1343.
25 S. Dalai, P. S. Mukherjee, E. Zangrando, F. Lloret and N. R. Chaudhuri, *J. Chem. Soc., Dalton Trans.*, 2002, 822–823.
26 R. Carballo, A. Castineiras, B. Covelo and E. M. Vazquez-Lopez, *Polyhedron*, 2001, **20**, 899–904.
27 S. M. F. Lo, S. S. Y. Chui, L. Y. Shek, Z. Y. Lin, X. X. Zhan, G. H. Wen and I. D. Williams, *J. Am. Chem. Soc.*, 2000, **122** 6293–6294.
28 J. Tao, M. L. Tong and X. M. Chen, *J. Chem. Soc., Dalton Trans.*, 2000, 3669–3674.
29 K. Seki, *Phys. Chem. Chem. Phys.*, 2002, **4**, 1968–1971.
30 X. J. Zheng, L. C. Li, S. Gao and L. P. Jin, *Polyhedron*, 2003, **23**, 1257–1262.
31 H. Liang, F. P. Liang, Z. L. Chen, R. X. Hu and K. B. Yu, *J. Indian Chem. Soc.*, 2001, **78**, 438–443.
32 C. Seward, N. X. Hu and S. N. Wang, *J. Chem. Soc., Dalton Trans.*, 2001, 134–137.
33 D. L. Long, A. J. Blake, N. R. Champness, C. Wilson and M. Schroder, *Chem.-Eur. J.*, 2002, **8**, 2026–2033.
34 D. L. Long, A. J. Blake, N. R. Champness and M. Schroder, *Chem. Commun.*, 2000, 1369–1370.
35 G. R. Choppin and D. R. Peterman, *Coord. Chem. Rev.*, 1998, **174**, 283–299.
36 O. Kahn, *Molecular Magnetism*, VCH Publishers, New York, 1993.